PROCEEDINGS OF SCIENCE

Relativistic Mean Field Model Constrained by Astrophysical Measurements

Bruno A. M. Soares,* **César H. Lenzi and Mariana Dutra**

Departamento de Física, Instituto Tecnológico de Aeronáutica,
Praça Marechal Eduardo Gomes, São José dos Campos, Brazil

E-mail: bmoura@ita.br, chlenzi@ita.br, marianad@ita.br

In this work, we present a preliminary study about constraints on saturation properties of nuclear matter using the Bayesian analysis method, where it was considered an equation of state (EoS) that allows $\omega - \rho$ interactions. Regarding the priors, we have used a uniform distribution on the values of saturation density, binding energy, effective mass, incompressibility, symmetry energy, and its slope at nuclear saturation density, whose ranges agree with the current literature. The posterior has been computed using the procedure of Bayesian inference, where observational data of neutron star masses and radii from gravitational wave event (GW170817) and the most recent published NICER events are employed. The results indicate lower values of L_0 for the EoS with $\omega - \rho$ interactions if compared to $\sigma^3 - \sigma^4$ ones, $65.4^{+18.1}_{-11.3}$ MeV and $78.8^{+8.0}_{-1.3}$ MeV respectively.

XV International Workshop on Hadron Physics (XV Hadron Physics) 13 -17 September 2021
Online, hosted by Instituto Tecnológico de Aeronáutica, São José dos Campos, Brazil

*Speaker

PoS(XVHadronPhysics)033

1. Introduction

The core of a Neutron Star (NS) is a few times denser than saturation density (ρ_0). There is no well-defined nuclear potential yet, so its properties are largely unknown. Laboratories experiments, such as the Large Hadron Collider (LHC at CERN), give us some descriptions of Equation of State (EoS) in symmetrical nuclear matter at saturation density. Using theoretical models, the EoS can be extrapolated to densities above ρ_0 and for asymmetrical matter, but it is very model-dependent.

With these EoSs, we can solve the Tolman-Oppenheimer-Volkoff (TOV) equations [1] to get a Mass-Radius diagram. Thus, once we have the measurements of masses and radii from some detectors, such as LIGO and NICER, it is possible to provide constraints on some EoS properties. In this scenario, we see that a better understanding about the EoS is essential for Nuclear Physics, to describe nuclear forces and structure, as well as Astrophysics, to understand the inside of a NS.

2. The Equation of State

The chosen Lagrangian for the present work is:

$$\begin{aligned}\mathcal{L} =&\bar{\Psi}(i\gamma^\mu\partial_\mu - M)\Psi - g_\sigma\sigma\bar{\Psi}\Psi - g_\omega\bar{\Psi}\gamma^\mu\omega_\mu\Psi - \frac{1}{2}g_\rho\bar{\Psi}\gamma^\mu\vec{\rho}_\mu\vec{\tau}\Psi + \frac{1}{2}(\partial^\mu\sigma\partial_\mu\sigma - m_\sigma\sigma^2)\\ &- \frac{A}{3}\sigma^3 - \frac{B}{4}\sigma^4 - \frac{1}{4}F^{\mu\nu}F_{\mu\nu} + \frac{1}{2}m_\omega^2\omega_\mu\omega^\mu - \frac{1}{4}\vec{B}^{\mu\nu}\vec{B}_{\mu\nu} + \frac{1}{2}m_\rho^2\vec{\rho}_\mu\vec{\rho}^\mu + \frac{1}{2}\alpha g_\omega^2 g_\rho^2\omega_\mu\omega^\mu\vec{\rho}_\mu\vec{\rho}^\mu\end{aligned} \tag{1}$$

We solve the Euler-Lagrange equations using the mean field approximation to get the fields equations and then we find the pressure (P) and energy density (ε) as a function of the baryonic density (ρ). For more details see [2].

$$\begin{aligned}\varepsilon =&\frac{1}{2}m_\sigma^2\sigma^2 + \frac{A}{3}\sigma^3 + \frac{B}{4}\sigma^4 - \frac{1}{2}m_\omega^2\omega_0^2 - \frac{1}{2}m_\rho^2\bar{\rho}_0{}^2 + g_\omega\omega_0\rho + \frac{g_\rho}{2}\bar{\rho}_0\rho_3\\ &- \frac{1}{2}\alpha g_\omega^2 g_\rho^2\omega_0^2\bar{\rho}_0{}^2 + \varepsilon_{cin}^n + \varepsilon_{cin}^p\end{aligned} \tag{2}$$

$$\begin{aligned}P =&- \frac{1}{2}m_\sigma^2\sigma^2 - \frac{A}{3}\sigma^3 - \frac{B}{4}\sigma^4 + \frac{1}{2}m_\omega^2\omega_0^2 + \frac{1}{2}m_\rho^2\bar{\rho}_0{}^2 + \frac{1}{2}\alpha g_\omega^2 g_\rho^2\omega_0^2\bar{\rho}_0{}^2\\ &+ P_{cin}^n + P_{cin}^p,\end{aligned} \tag{3}$$

where

$$\varepsilon_{cin}^{p,n} = \frac{\gamma}{2\pi^2}\int_0^{k_{F\,p,n}} k^2(k^2 + (M^*)^2)^{1/2}dk, \quad \text{and} \quad P_{cin}^{p,n} = \frac{\gamma}{6\pi^2}\int_0^{k_{F\,p,n}} \frac{k^4}{(k^2 + (M^*)^2)^{1/2}}dk. \tag{4}$$

There are six coupling constants to adjust: $\frac{g_\sigma^2}{m_\sigma^2}$, $\frac{g_\omega^2}{m_\omega^2}$, $\frac{g_\rho^2}{m_\rho^2}$, $\frac{A}{g_\sigma^3}$, $\frac{B}{g_\sigma^4}$, and α. Therefore, six parameters are needed for the EoS, which are: the effective mass (m_0^*), incompressibility (K_0), saturation density (ρ_0), symmetry energy (J), binding energy (E_0) and the slope of the symmetry energy (L_0), all of them calculated at saturation density in symmetric nuclear matter (SMN).

3. Bayesian Analysis

The probability distribution of a set of parameters θ, once it is given a data D, is called posterior density function, $P(\theta|D)$, and it is inferred by the Bayes' Theorem,

$$P(\theta|D) = \frac{P(D|\theta)P(\theta)}{P(D)}, \tag{5}$$

where $P(D|\theta)$ is the Likelihood, that is the probability of getting D given θ. $P(\theta)$ is the prior probability, and $P(D)$ is known as the evidence and it can be treated as a normalization factor.

As we know, different types of priors may alter the posteriors. For the sake of simplicity we adopted a uniform distribution with the ranges of m_0^*, K_0, ρ_0, J, and E_0 inspired in results of laboratory experiments and which have been used previously in the work [3]. For the ranges of the slope (L_0) we take the intersection limit of four recent studies, based on the data of PREX-2 collaboration.[4–7]. These ranges can be seen in Table 1.

Range	m_0^*	$K_0(MeV)$	$\rho_0(fm^{-3})$	$J(MeV)$	$E_0(MeV)$	$L_0(MeV)$
min	0.7	200	0.14	28	-16.5	50.0
max	0.8	300	0.16	35	-16.0	110.0

Table 1: Ranges of the parameters used in the priors.

To calculate the Likelihood, $P(D|\theta)$, of a given set of parameters θ, we follow the procedure in [3]. Firstly, the corresponding EoS to the set of bulk parameters must be calculated. Thereby, we need to solve the TOV equations with multiple values of central density to get a mass-radius curve. The point where the highest probability occurs is the probability that we assign as the value for the Likelihood. We repeat this process for every one of the sources and the joint likelihood will be: $P(data|\theta) = \prod_{i=1}^{n} P(D_i|\theta)$.

In this preliminary study we used sixteen sources ($n = 16$), one of them was the recently published data from NICER which estimated the radius of the $(2.08 \pm 0.07)\mathrm{M}_\odot$ source PSR J0740+6620 to be $13.7^{+2.6}_{-1.5}$ km [8]. From the work of Özzel (2016) [9], we used eleven sources, six thermonuclear burster sources: 4U1820-30, SAX J1748.9-2021, EXO 1745-248, KS 1731-260, 4U 1724-207, 4U 1608-52; and five qLMXB sources: M13, M30, NGC 6304, NGC 6397 and ωCen. We also used two sources from the gravitational wave event GW170817 [10]; the source 4U 1702–429 which its mass and radius was inferred by Nättilä et al.(2017) [11]; and lastly, the mass and radius of PSR J0030+0451, from NICER collaboration [12].

4. Results

The joint Probability Density Function (PDF) of the parameters and their most probable values within 68% Confidence Interval (CI) can be seen in figure 1. We see that K_0, ρ_0 and L_0 tend to have their most probable value towards the edge of their boundaries. J and E_0 have a uniform distribution, which does not give us new constraints about its values. This may indicate that the J and L_0 could be correlated, therefore in future work, we have to change one of these parameters since we need the parameters to be independent of each other. Notice that $\omega - \rho$ EoSs gives significant lower

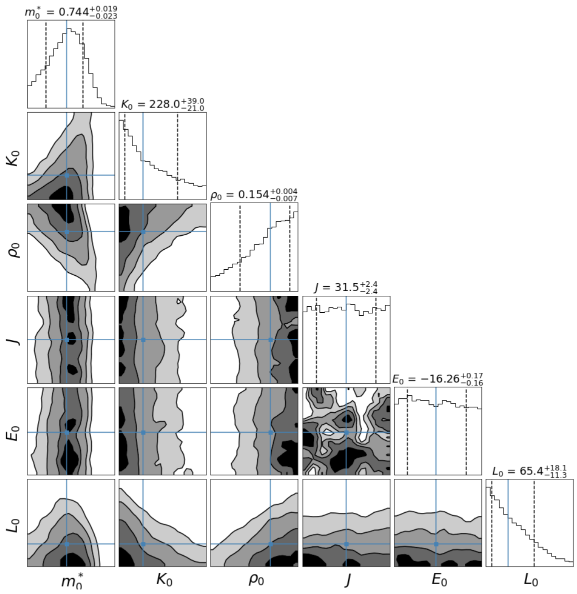

Figure 1: Posterior of the bulk parameters for an EoS that allows $\omega - \rho$ Interactions. The blue line is the most probable value and the dashed lines are the values at 2σ (68% CI).

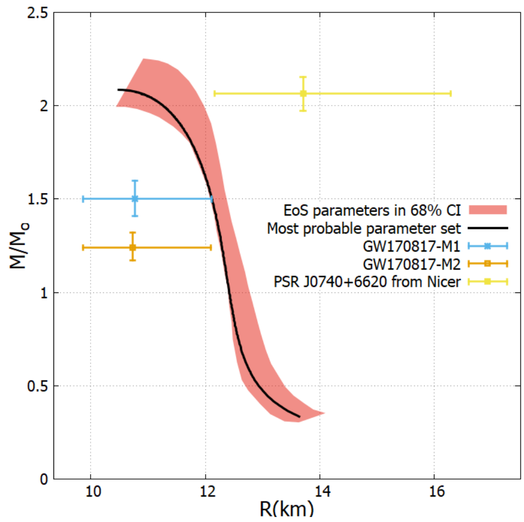

Figure 2: Mass-radius diagram corresponding to the most probable EoS parameters.

values of m_0^* and L_0 compared with $\sigma^3 - \sigma^4$ ones, $65.4^{+18.1}_{-11.3}$ MeV and $78.8^{+8.0}_{-1.3}$ MeV respectively (For comparison, see Figure 1 of [3]). The lower value of the slope is directly related with the last term of the Lagrangian (1) which corresponds to the $\omega - \rho$ interactions. This may be in line with new results from PREX-II experiments [7], which may indicate that the interaction between mesons ω and ρ do indeed occur at nuclear densities. It is also worth noting that the resulting values of all parameters are in agreement with existing experiments.

The mass-radius curve shown in figure 2 corresponds to the EoS with the most probable parameters. We can see that the curve has a hard time being compatible with LIGO sources and PSR J0030+0451 because the latter has a much higher mass than most of the neutron stars observed. Furthermore, we see that the most probable configuration lies at the edge of the 68% Confidence Interval, which correlates with the trend of lower values of K_0 and L_0.

5. Conclusion

This preliminary study presented how recent observations of NS masses and radii, such as NICER [8], in the light of new studies on the PREX-2 experiments [4–7], can give us additional information about the properties of the nuclear matter of the NS using Bayesian Analysis. To do this, we used observational data from 16 different sources that gave us new constraints on the possible values of the bulk parameters of SNM, which are shown in figure 1. The chosen type of EoS resulted in lower values of L_0, but they still agree with results from PREX-II studies. Due to its probabilistic nature, Bayesian Inference will get more precise as more observational data are incorporated. Future works will rely on new data sources and different types of prior distribution will be applied.

Acknowledgments

This work is a part of the project INCT-FNA Proc. No. 464898/2014-5. It is also supported by Conselho Nacional de Desenvolvimento Científico e Tecnológico (CNPq) under Grants 433369/2018-3, and 308528/2021-2 (M. D.). We also acknowledge Fundação de Amparo à Pesquisa do Estado de São Paulo (FAPESP) under Thematic Project No. 2017/05660-0 (M. D. and C. H. L.) and Grant No. 2020/05238-9 (M. D. and C. H. L.). The authors also thank LAB-CCAM from ITA for computational support. The authors acknowledge POWER DATA TECNOLOGIA LTDA for providing a technological environment (big data & analitics) for data processing.

References

[1] J.R. Oppenheimer and G.M. Volkoff, Phys. Rev. **55** (1939) 374.

[2] M. Dutra, O. Lourenço, S.S. Avancini, B.V. Carlson, A. Delfino, D.P. Menezes et al., Phys. Rev. C **90** (2014) 055203.

[3] S. Traversi, P. Char and G. Pagliara, The Astrop. J. **897** (2020) 165.

[4] SπRIT Collaboration collaboration, Phys. Rev. Lett. **126** (2021) 162701.

[5] B.T. Reed, F.J. Fattoyev, C.J. Horowitz and J. Piekarewicz, Phys. Rev. Lett. **126** (2021) 172503.

[6] T. Yue, L. Chen, Z. Zhang and Y. Zhou, arXiv **10.48550/arXiv.2102.05267** (2021) .

[7] R. Essick, I. Tews, P. Landry and A. Schwenk, Phys. Rev. Lett. **127** (2021) 192701.

[8] M.C. Miller, F.K. Lamb, A.J. Dittmann, S. Bogdanov, Z. Arzoumanian, K.C. Gendreau et al., The Astrop. J. Lett. **918** (2021) L28.

[9] F. Özel, D. Psaltis, T. Güver, G. Baym, C. Heinke and S. Guillot, The Astrop. J. **820** (2016) 28.

[10] The LIGO Scientific Collaboration and the Virgo Collaboration collaboration, Phys. Rev. Lett. **121** (2018) 161101.

[11] Nättilä, J., Miller, M. C., Steiner, A. W., Kajava, J. J. E., Suleimanov, V. F. and Poutanen, J. , A&A **608** (2017) A31.

[12] T. Riley, A. Watts, S. Bogdanov, P. Ray, R. Ludlam, S. Guillot et al., Zenodo **10** (2019) .